

Nanostructured Metal Oxides for High-Temperature Gas Sensing: Structural Stabilization in Porous Metal Oxides

Dominik Klaus, Michael Tiemann, Thorsten Wagner
 Universität Paderborn, Naturwissenschaftliche Fakultät, Department Chemie
 Warburger Straße 100, D-33098 Paderborn, Germany
 dominik.klaus@uni-paderborn.de

Abstract

As recently shown, nanostructured SnO₂ and In₂O₃ prepared by nanocasting exhibit higher thermal structural stability than their non-ordered counterparts [1,2]. In the presented work we will show a correlation of the thermal stability with the crystallite size of the nanostructure. In₂O₃ is utilized as model material since preparation of nanocast phases with variable crystallite sizes is possible [3] and it is a qualified sensing material [4]. Two samples with different crystallite sizes but otherwise comparable structural features are thermally treated stepwise in a temperature range between 250°C and 700°C. The specific surface area (BET) is observed as a probe for the structural integrity of the material. Results show a shift of the mesostructure breakdown (steep decrease in BET surface area) to higher treatment temperatures for the sample with the larger lateral crystallite size. This breakdown is attributed to a coalescence-based growth mechanism. A linear decrease in surface area observed for both samples is assigned to Ostwald ripening which leads to a smoothing of the inner surfaces and a sealing of the micropores in the walls of the nanocast material.

Key words: metal oxide, nanocasting, mesoporous, thermal stability, Indium Oxide, high temperature

Introduction

Signal stability of semiconducting gas sensors depends strongly on the structural parameters of the sensing layer [5]. Most nanostructures are not applicable as high-temperature sensing layers because of their structural instability at elevated temperature. Ordered mesoporous metal oxides synthesized by nanocasting, however show higher structural stabilities as compared to other materials with similar lateral dimensions in the nanometer range [1,2]. They also offer a good and reproducible gas interface due to their unique structural features [6]. To gain a deeper understanding of the stabilization mechanism a model based on two distinct processes for particle growth, namely coalescence [7] and Ostwald ripening [8], was proposed (see figure 1). Since the vapor pressure of metal oxides is very low, ripening via gas-phase transport is only a minor effect and coalescence is dominating. The nanocasting process typically involves a high temperature pre-treatment procedure of the material prior to removal of the rigid structure matrix. This often leads to pore walls with high-aspect ratio crystallites. Along the wall the crystallites can be as large as 30 nm whereas their thickness is below 10 nm; this dimension is suitable for gas sensing. Thermodynamically

though, these nanostructures behave more like 30 nm particles. The thermal energy needed for re-orientation is higher than for 10 nm particles and therefore the stability is increased.

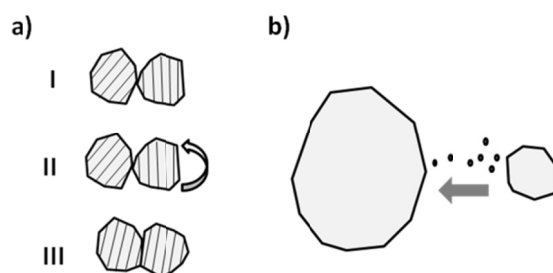


Fig. 1. Nanoparticle growth mechanisms: a) coalescence of non-aligned grains (I), crystal planes rearrange (II) and allow for fusion (oriented attachment) of the particles (III); b) Ostwald ripening: large grains grow at the expense of smaller grains via the gas phase.

To test this model samples with different crystallite sizes are synthesized and their thermal stability is investigated.

Experimental

A mesoporous silica matrix (KIT-6 [9]) was impregnated with molten indium nitrate pentahydrate (In(NO₃)₃·5H₂O; Sigma-Aldrich). After 24h at 80°C in a muffle-type furnace

indium nitrate was converted to indium oxide in a tube furnace at a temperature of 300°C with a heating rate of 2°C/min. For the variation of the crystallite size the sample was kept in an open vessel and a closed custom-built reactor respectively. The open vessel allows the air stream to carry the reaction gases away from the sample whereas the closed vessel prevents the nitrous gases generated during the conversion from being immediately removed. After conversion the silica matrix was removed by three times leaching with aqueous NaOH (5 mol L⁻¹) at 60°C for 1h. After each step the product was washed with distilled water until a pH of 7 was reached. The mesoporous indium oxide was finally dried in a muffle oven at 60°C for 24h.

The resulting samples were characterized with scanning electron microscopy (SEM), N₂physisorption and powder X-ray diffraction (PXRD).

Crystallite Size

The lateral size of the crystalline domains of mesoporous In₂O₃ was varied by controlling the atmosphere during conversion.

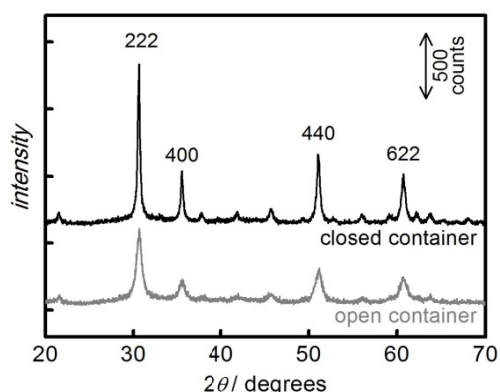


Fig. 2. Powder X-ray (PXRD) diffraction patterns of ordered mesoporous In₂O₃ prepared in a closed (red) and in an open (blue) vessel, respectively.

Figure 2 shows the PXRD diffraction patterns of the samples converted in an open and a closed reaction vessel. The sample prepared in the closed vessel exhibits narrower peaks.

Tab. 1. Crystallite sizes of mesoporous In₂O₃ according to peak width analysis by Scherrer's method for various crystallographic directions.

	In ₂ O ₃ crystallite size (in <i>h k l</i> direction) / nm			
	222	400	440	622
open vessel	13.4	14.2	11.6	11.7
steel reactor	30.1	27.9	21.1	19.3

The crystallite size estimated by utilizing Scherrer's equation is twice as large size in all crystallographic directions as for the sample prepared in the closed vessel (see table 1).

Porosity and Particle Structure

The pore size distribution (BJH), the pore volume and the specific surface area (BET) determined by N₂physisorption show fundamental disparities. The sample converted in the open vessel (small crystals) exhibits a specific surface area of 90.2 m²g⁻¹. The pore volume is 0.38 cm³g⁻¹ and the pore size distribution shows three peaks at 4.37, 5.67 and 12.58 nm respectively (see figure 3).

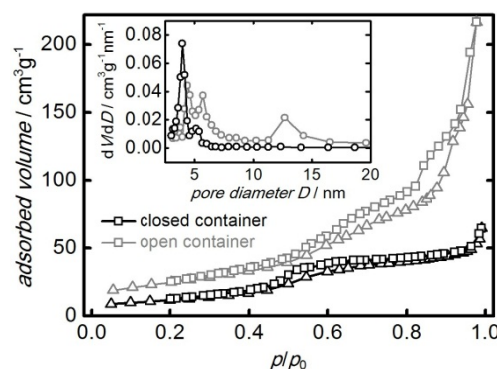


Fig. 3. N₂physisorption isotherms and pore diameter distributions of In₂O₃ prepared in a closed and in an open reactor.

The sample converted in the closed steel reactor (large crystallites) shows a distinct pore size distribution peak at 3.95 nm. The specific surface area (43.3 m²g⁻¹) as well as the pore volume (0.38 cm³g⁻¹) are smaller compared to the open-vessel sample.

We attribute the described differences in porosity to a higher surface roughness of the pore walls caused by smaller crystallite sizes in the open vessel sample.

The overall sizes of the mesoporous particles were also found to be dependent on the synthesis process.

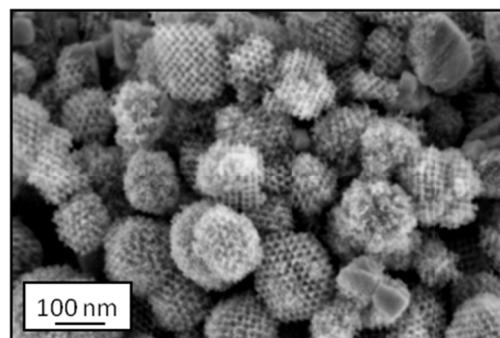


Fig. 4. Scanning electron microscopy (SEM) image of an In₂O₃ sample converted in an open vessel.

For the open vessel the ordered mesoporous particles have diameters of ca. 200 nm (see figure 4) whereas particles of the sample converted in the closed reactor are more than 1 μm in diameter (not shown). However, the size of the mesostructured particles is likely not to influence the stability of the mesopore system.

Thermal Stability

After analyzing the structural properties of the two mesoporous samples the structural stability after treatment at variable temperature was investigated. The BET surface area is used as a measure for the quality of the mesoporous structure. Figure 5 shows the change in surface area after treatment in the range of 250°C and 700°C as a percentage of the initial surface area. An approximately linear decrease is observed up to 500°C for the sample converted in the open vessel (small crystallites) and up to 550°C for the sample converted in the closed container (large crystallites), respectively.

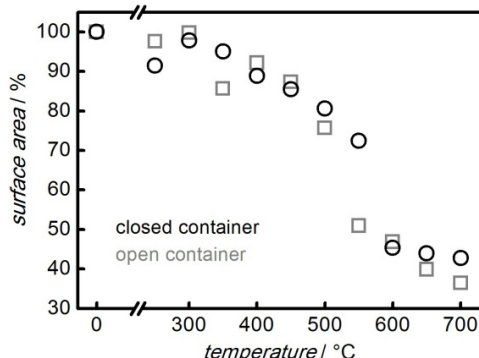


Fig. 5. Decrease of the BET surface area upon treatment at variable temperature for both mesoporous In_2O_3 samples.

Above these temperatures a sudden steep decrease in the surface area is observed. For the sample with the large crystallites the temperature for this effect is ca. 50°C higher than for the sample with small crystallites.

This behavior can be explained by means of the proposed model. The linear decrease is attributed to ripening effects via the gas phase (Ostwald ripening). This leads to a smoothing of the pore walls and therefore to a slight decrease in the specific surface area. The steep decrease, on the other hand, is caused by the breakdown of the mesoporous structure which is caused by growth via coalescence.

Conclusion

Two ordered, mesoporous In_2O_3 samples with different crystallite size were synthesized by varying the reaction vessel during the conversion of indium nitrate in a nanocasting route. Temperature treatments of the products and analysis of the morphological properties

exhibit higher structural stability for the sample with larger crystallites, which is in accordance with the proposed model based coalescence as the main effect for mesopore structure breakdown. However, in addition to crystallite size other structure-related parameters, e.g. the specific surface area, may play a role; this will be subject of future investigation.

Acknowledgements

We thank the DFG (WA 2977/1-1) for financial support and Sabrina Amrehn for assisting at the synthesis of the In_2O_3 -samples.

References

- [1] Waitz, T., Becker, B., Wagner, T., Sauerwald, T., Kohl, C.-D., Tiemann, M., Ordered Nanoporous SnO_2 Gas Sensors with High Thermal Stability, *Sensors and Actuators B: Chemical* 150, 788–793 (2010); doi: 10.1016/j.snb.2010.08.001
- [2] Waitz, T., Wagner, T., Sauerwald, T., Kohl, C.-D., Tiemann, M., Ordered Mesoporous In_2O_3 : Synthesis by Structure Replication and Application as a Methane Gas Sensor, *Advanced Functional Materials* 19, 653–661 (2009); doi: 10.1002/adfm.200801458
- [3] Sun, X., Shi, Y., Zhang, P., Zheng, C., Zheng, X., Zhang, F., Zhang, Y., Guan, N., Zhao, D., Stucky, G.D., Container Effect in Nanocasting Synthesis of Mesoporous Metal Oxides: *Journal of the American Chemical Society, J. Am. Chem. Soc.* 133, 14542–14545 (2011); doi: 10.1021/ja2060512
- [4] Wagner, T., Sauerwald, T., Kohl, C.-D., Waitz, T., Weidmann, C., Tiemann, M., Gas Sensor Based on Ordered Mesoporous In_2O_3 : Proceedings of VI International Workshop on Semiconductor Gas Sensors - SGS 2008, *Thin Solid Films* 517, 6170–6175 (2009); doi: 10.1016/j.tsf.2009.04.013
- [5] Yamazoe, N., New Approaches for Improving Semiconductor Gas Sensors, *Sensors and Actuators B: Chemical* 5, 7–19 (1991); doi: 10.1016/0925-4005(91)80213-4
- [6] Tiemann, M., Porous Metal Oxides as Gas Sensors, *Chem. Eur. J.* 13, 8376–8388 (2007); doi: 10.1002/chem.200700927
- [7] Huang, F., Zhang, H., Banfield, J.F., Two-Stage Crystal-Growth Kinetics Observed during Hydrothermal Coarsening of Nanocrystalline ZnS , *Nano Letters* 3, 373–378 (2003); doi: 10.1021/nl025836+
- [8] Adamson, A.W., Gast, A.P. *Physical chemistry of surfaces*, 6th ed; Wiley: New York, 1997; ISBN: 0471148733
- [9] Kleitz, F., Choi, S.H., Ryoo, R., Cubic Ia3d Large Mesoporous Silica: Synthesis and Replication to Platinum Nanowires, Carbon Nanorods and Carbon Nanotubes, *Chem Commun (Camb)*, 2136–2137 (2003); doi: 10.1039/B306504A